Coronal Seismology

Laurel Farris
New Mexico State University
laurel07@nmsu.edu

ABSTRACT

Coronal seismology involves the investigation of magnetohydrodynamic (MHD) waves and oscillatory phenomena that arise in the solar corona. Properties of the observed modes are largely dependent on their environment, and therefore can be used to extract atmospheric parameters that are otherwise difficult to observe. The general theory behind MHD phenomena is investigated here, along with the characteristics of different modes and the information that can be extracted from them. A few methods are applied to data from the *Atmospheric Imaging Assembly* (AIA) instrument on the *Solar Dynamics Observatory* (SDO).

Subject headings: Sun: corona Sun: oscillations Sun: seismology

1. Introduction

Properties of the corona that are difficult to measure directly can be extracted from observations of properties of MHD waves and oscillations (Verwichte et al. (2013)).

The basic concepts of MHD waves and oscillations are described in §2, and §3 covers several MHD modes in detail. Many of the techniques employed in coronal seismology were applied to AIA data; a description of the project and the results are presented in §5 and §6. Conclusions and future work are discussed in §7.

2. Basic MHD

2.1. Types of Waves

In general, MHD waves are divided into two categories: Alfvén waves and magnetoacoustic waves. Magnetoacoustic waves are further subdivided into slow-mode and fast-mode (Aschwanden (2004)). The slow-mode waves have phase speeds roughly equal to the sound speed in the medium in which they reside, analogous to typical acoustic waves, or sound waves. MHD studies usually focus on the fast-mode. Fast-mode magnetoacoustic waves have phase speeds comparable to the Alfvén speed, or $\omega/k \approx v_A$ (Aschwanden et al. (1999)). Two common fast modes in the corona are the asymmetric *kink* oscillations and symmetric *sausage* oscillations, which are discussed in more detail in §3.1 and §3.2, respectively.

The categories of MHD waves and oscillations can be best understood by their relative speeds. Figure 1 shows the wave speeds relative to the internal and external Alfvén and sound speeds.

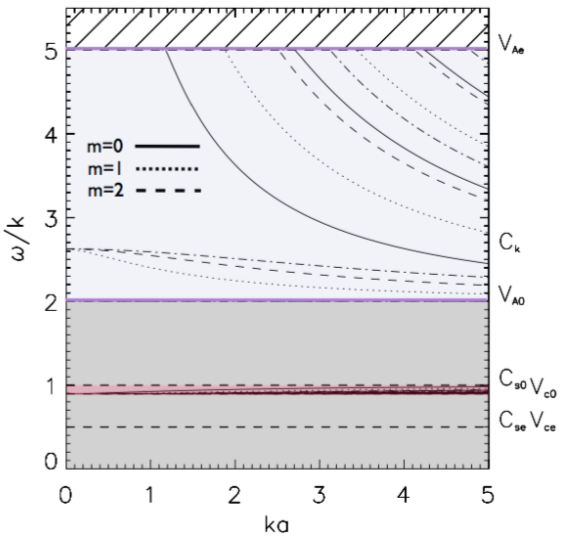

Fig. 1.— text (Image credit: Nakariakov & Verwichte (2005))

The sound speed in a medium is determined by thermal properties: the thermal pressure and the mass density of the medium. It is given by:

$$c_s = \sqrt{\frac{\gamma}{\rho}} \tag{1}$$

The Alfvén speed, on the other hand, is determined by the magnetic pressure:

$$c_A = \frac{B}{\sqrt{4\pi\rho}} \tag{2}$$

Each MHD mode is characterized based on a number of qualities, such as its wavelength, period, lifetime, speed, and whether it is propagating or standing, fast or slow, longitudinal or transverse, etc. The driving mechanisms that give rise to each mode can differ depending on these qualities and the environment in which the modes reside, and is one of the important MHD topics under investigation, along with the damping mechanism (Aschwanden et al. (1999)).

2.2. Equations and Models

MHD waves are often modeled with a cylindrical flux tube embedded in a magnetic field.

[cylindrical model, equations of ideal MHD, etc.]

$$\xi(x) = \xi(r)e^{i(kx+m\phi)} \tag{3}$$

For kink oscillations, m=1, and for sausage modes, m=0.

There are several equations for ideal MHD from which the dispersion relations are derived (I think).

2.3. Excitation and Damping Mechanisms

2.3.1. Resonant Absorption

(The following is straight from (Nakariakov & Verwichte (2005)), so it needs to be re-worded and expanded at some point). If the frequency of a wave falls within one of two types of MHD continua (namely, the Alfvén or cusp continua), a resonance will occur in the location where math happens. In the cylinder model, this location is a shell at radius r. In the Alfvén continuum, the Alfvén wave is the mode that is resonantly excited and dissipates in the corona. This is one of the processes thought to contribute to the heating of the corona. It involves the conversion from a collective mode to a local mode, which occurs at a timescale much shorter than that of the dissipative damping. To analyze this mathematically, equations of ideal MHD cannot be used because dissipation effects must be taken into account.

2.3.2. Phase Mixing

Another effect associated with wave modes from MHD continua is called phase mixing, and is also a possibly mechanism behind the heating of the corona.

2.4. Observation Techniques

Flux tubes (coronal loops), Doppler shift and intensity variations, density variations, velocity and magnetic field values, etc. Coronal loops are density inhomogeneities in the corona, where the (low-β) plasma is "frozen-in" along the magnetic field lines whose feet are anchored in the photosphere.

3. Types of MHD Modes

3.1. Kink Oscillations

Kink oscillations are directly observed in coronal loops in extreme ultraviolet (EUV) wavelengths. They characterize the spacial oscillations that occur over the surface of the loop, perpendicular to the direction traversed by the length of the loop (Nakariakov & Verwichte (2005)). Kink oscillations generally are not accompanied by intensity variations; they displace the axis of the magnetic structure in which they propagate, but the cross-section of the waveguide remains roughly the same. Kink oscillations occur in the "long-wavelength regime", which is defined by the product of the wavenumber and the cross-section of the coronal loop being much less than 1 ($ka \ll 1$). In other words, the *wavelength* of the oscillation is much *greater* than the cross-section of the waveguide. The phase speed is just above the Alfvén speed within the loop, and the period of the oscillation is expected to be between $\sim$ 2 and 20 minutes (Aschwanden (2004)). Observations of kink oscillations are important to solar physics as the magnetic field strength can be derived from the period.

Due to a lack of sufficient instrumentation, spatial variations such as those caused by kink oscillations were not resolved until the launch of TRACE. Some of the first results from preliminary TRACE data were produced by Aschwanden et al. (1999) to investigate the oscillations present in coronal loops. Using 171 Å data, they modeled five loops that accompanied a class M4.6 solar flare in July of 1998. At this point, many MHD modes were characterized in theory

The observations had enough qualities characteristic of fast kink modes, including the spatial displacements characteristic of this asymmetrical mode, to identify these oscillations as kink modes.

An average period of $T = 269 \pm 6$ seconds, or roughly 4.5 minutes, was obtained, which fit well with the theoretical period for kink oscillations. The absence of any phase shift along the length of the loops revealed that these were *standing waves*, with nodes located at the loop footpoints. The ability to identify kink modes has great significance for solar physics due to a correlation between the oscillation period, T, and the magnetic field strength, B, of the loop:

$$T \propto \frac{L}{\sqrt{n}} B \tag{4}$$

where L is the loop length and n is the number density, both of which can be estimated from known coronal conditions.

More recently, Pascoe et al. (2015) investigated the driving mechanism behind the production, and damping of the kink mode. This was found to occur on rapid timescales for both standing and propagating kink modes, both of which are consistently found throughout the solar coronal. However, it was unclear what was causing these modes to damp out so quickly. The gravitational stratification of the atmosphere could have the effect in *increasing* the velocity amplitude, thus reducing the attenuation caused by mode-coupling.

They compared two possible functional forms of the damping profile of the driver: that of a Gaussian and an exponential form. The gaussian was a potential form of the amplitude variation at a lower height (z), while the variation at higher z took the form of an exponential. While the noise level of the data was too high to distinguish between the two forms, the simulations followed the form of a Gaussian.

They also considered the effect of the spatial profile of the driver itself on the excitation and subsequent damping of the kink waves. Two different possibilities were explored here: the effect of a "highly structured" driver including only the exponential damping profile, which they found to be unrealistic. The effects of small-scale (less than the size of the loop cross-section) of eddies and photospheric motions around the footpoints of the loops were also considered. These motions can excite kink modes along the length of the coronal loop, but not as efficiently as those produced by larger scale motions. These motions are what determine the properites of the observed modes. The observed damping of the kink mode was found to be a result of mode-coupling and subsequent energy transfer from the characteristic transverse motions of the kink mode, to azimuthal motions. The period observed by *CoMP* was centered around 5 minutes, fitting within the expected kink period of 2-20 minutes. The phase speed was around 0.6 Mm s^{-1}, leading to a calculated wavelength of about 180 Mm.

3.2. Sausage Oscillations

In contrast to kink oscillations, sausage oscillations do not displace the axis of the structure in which they reside. However, they do cause a periodic change in the cross-section of the waveguide, and hence are observable through changes in intensity (and therefore density, due to flux conservation). Sausage oscillations only exist shortward of the long wavelength cutoff, where the wavelength is comparable to the cross-section of the loop in which they oscillate. Therefore they can only exist in loops that are "sufficiently thick and dense" (Yuan et al. (2013)).

Lopin & Nagorny (2015) plotted the changes in intensity and cross-sectional area for sausage oscillations in photospheric pores extending up through the solar atmosphere. They used the general cylinder model for the pores, though it is more likely that the cross-sectional area of the waveguide increases with height as the temperature increases and density decreases. Sausage waves are characterized by a change in the cross-section, but no displacement of the loop axis. They occur on much shorter timescales than kink waves. The relationship between pore size and intensity can indicate

Morton et al. (2011) investigated oscillations associated with magnetic pores, which are essentially small sunspots with an upper limit of about 1700 km in diameter and consist of an umbra, but no penumbra (cite class notes?). These features have high magnetic strength ($\sim$ 1700 G) in the photosphere and expand in diameter as the height above the photosphere increases into the chromosphere. As magnetic flux is always conserved, observing the size of these features in the upper layers of the atmosphere can reveal their size in the photosphere, which is not as easily observable. However, this requires knowledge of their magnetic strength in the atmosphere as well.

These pores act as a waveguide (much like the way coronal loops act as a waveguide). Observations along the line of sight reveal periodic changes in intensity due to the change in cross-section characteristic to sausage modes. These two variations are 180° out of phase, as an increase of surface area corresponds to a decrease in density, and hence, a decrease in intensity. The observed period for These modes was about 30-450 seconds, and they were considered as a possible heating mechanism for the corona. However, some wavelengths are reflected at the transition regions, while other make it through, and the ones that do make it through are not abundant enough to heat the corona to the temperatures that are observed.

3.3. Acoustic Oscillations

The relatives periodicities of acoustic oscillations were recognized as important characteristics, and modeled by Roberts et al. (1984). They recognized magnetoacoustic oscillations as a useful way to determine other properties of the solar atmosphere.

Srivastava & Dwivedi (2010) used intensity oscillations of a few different ionization species to pinpoint the origin and progression of magnetoacoustic waves between bright points in the photosphere, through the transition regions, and up into the corona. The time series of intensity oscillations was converted into a power spectrum, and periodicities were extracted using wavelet analysis and periodograms (note here on what exactly these are?). The periods they derived ($\sim 263\pm80$ s for the He II 256.32 Å emission line and $\sim 241\pm60$ s for the Fe XII 195.12 Å emission line) were close to the 5-minute global oscillations of the sun.

3.4. Propagating Acoustic Waves

The MHD modes that have been discussed up to now are considered *standing* modes: waves with nodes in a fixed position, such as the footpoints of coronal loops that are anchored in the photosphere. These are referred to as *oscillations*. In contrast, *propagating* waves have nodes that move with time (though two propagating waves traveling in opposite directions can have a net result of a single, standing oscillation; see Aschwanden (2004), ch. 8).

Standing acoustic waves are primarily seen in closed coronal loops, while propagating waves have been observed in both closed (where the wave damps out before reaching the other footpoint; see Roberts et al. (1984)) and open structures. Waves with propagations speed much lower than the local Alfvén speed, are categorized as slow magnetoacoustic waves. These waves travel along magnetic field lines at speeds roughly equal to the local sound speed. The changes in intensity along the same location as these waves propagate in time are mapped side by side to give time-distance information. The period, wavelength, propagation speed, and amplitude can all be derived using this method. Since the local sound, c_s is related to temperature, T, as

$$c_s \propto \sqrt{T} \tag{5}$$

a difference in observed propagation speeds implies a changing temperature profile in the transverse direction across the loop. (Nakariakov & Verwichte (2005)).

Propagating acoustic waves are generally observed as "propagating disturbances" awaiting further diagnoses of magnetoacoustic waves, whose amplitudes are rather weak, requiring careful, detailed data analysis to acquire good signal-to-noise (S/N).

One of the first studies to analyze simultaneous observations at different wavelengths was carried out by Robbrecht et al. (2001) using data from two different instruments: the Extreme ultraviolet Imaging Telescope (EIS) on the Solar and Heliospheric Observatory (SOHO) and the Transition Region And Coronal Explorer (TRACE). These wavelengths, along with their corresponding ions emitting at those wavelengths, the temperature, and other relevant quantities from the study are given in table 1. Both instruments observed AR

instrument	EIT	TRACE
ion	Fe XII	Fe IX
wavelength	195 Å	171 Å
cadence	15 s	25 s
temperature	1.6 MK	1 MK
sound speed	192 km s^{-1}	152 km s^{-1}
propagation speed	110 km s^{-1}	95 km s^{-1}

Table 1: Relevant quantities from Robbrecht et al. (2001)

8218, where the presence of "weak transient disturbances" were revealed, and later classified as slow, propagating magnetoacoustic waves, with speeds that varied between 65 and 150 km s^{-1}. The expression for the formal sound speed of the ambient region was given by

$$c_s = 152\ \sqrt{T}\ \mathrm{m\ s^{-1}} \tag{6}$$

where T is in units of Kelvin. This was compared to the observed speed of the propagating wave, which was derived from the slope of the "ridges" on each of the four time-distance plots. The propagation speed of each wave was slightly ($\sim$ same order of magnitude) lower than the local sound speed. This difference was due to the angle between the loop and the plane of the sky against which the observations were made. The amount of time for a disturbance to pass a particular point was determined to be $\sim$ 169 s from the TRACE data. As both observations targeted the same wave, the significance of the differing speeds for each observation indicated a temperature gradient in the loop itself, indicating either a bundle of loop threads that make up a single loop, or a number of concentric shells that make up a single loop.

A similar analysis in multiple wavelengths was carried out by Uritsky et al. (2013), using about 6 hours of observational data from the Atmospheric Imaging Assembly (AIA) on the Solar Dynamics Observatory (SDO). In addition to these observations, they introduced the "surfacing transform technique" in order to address the difficulty in extracting information from these low-amplitude waves amidst the noise (a typical signal-to-noise (S/N) ratio was $\sim$ 0.1 %). (more information about this technique here?) This method involved the resonant behavior of "surfing signals", revealed during quasi-periodic disturbances.

This technique was applied to the lines at 131 Å, 171 Å, 193 Å, and 211 Å, over the active region (AR) NOAA AR 11082, where no sunspots were seen to be present and the flares were relatively low-energy. They found the same relationship between sound speed and temperature as shown in equation 5, though the driving mechanism for these disturbances was uncertain. The observed propagations were travelling primarily in the upward direction away from the footpoint, at speeds of about 40 to 180 km s^{-1} and periodicities between 4 and 8 minutes over all four channels.

3.5. Propagating Fast Waves

Propagating waves with speeds greater than (?) are categorized as fast waves (or some other definition; Nakariakov & Verwichte (2005) is not clear on this).

One type of fast propagating wave is the *Moreton* wave. These tend to emerge as a result of energetic flares and CMEs and only last for about 10 minutes (Asai et al. (2012)). They travel in very specific directions, as opposed to other waves that can be isotropic (source and better wording). They were described as the intersection of MHD fast waves shock-propagating between the chromosphere and corona, and are observed in Hα. While they are rarely observed, their counterparts can be seen in the corona in the form of EIT waves (named after the *EUV Imaging Telescope* on the *Solar and Heliospheric Observatory*).

Asai et al. (2012) observed a Moreton wave along with the (possibly) corresponding EUV wave in the corona. These waves were triggered by a class-X6.9 flare from AR NOAA 11263. The coronal wave was possibly the fast counterpart of the EIT wave. This was questionable due to the difference in the observed velocity between the two. The EIT wave had a velocity of 200-400 km s^{-1} and lasted for about 45-60 minutes, while the Moreton wave had a velocity between 500 and 1500 km s^{-1} and only lasted for 10 minutes. It was possible that the coronal wave decelerated, resulting in a lower velocity, but the authors seemed to think that this was not the case. EIT waves propagate isotropically while Moreton waves can only travel in restricted angles. The Morton wave was observed in Hα by the *SMART* telescope, as well as in 195 Å and 304 Å by *STEREO*, and in 193 Å by *AIA* (FeXII, at a temperature T=$10^{6.1}$ K).

The three main observations made here were:

- (MHD) EUV fast coronal waves
  - bright - Moreton wave
  - faint - Not associated with the Moreton wave
- Slow, bright EUV wave (A typical EIT wave)
- Filament and prominence oscillations

The lifetime of the Moreton wave was ~ 6 minutes, with an average velocity of $\langle v \rangle = 760$ km s^{-1}. The wave associated with the filament had $v = 300$ km s^{-1}.

Another investigation of propagating fast waves was carried out by Yuan et al. (2013). They observed intensity perturbations of "quasi-periodic propagating fast magnetoacoustic wave trains" associated with AR 11227. These wave trains appeared $\sim$ 110 Mm from the center of the flare, 2.2 minutes after the flare occurred. They were only visible in the AIA 171 Å bandpass, suggesting a location restricted to a certain height range above the photosphere. They derived an average velocity of 833 km s^{-1}, which is in the Alfvén range. Three wavetrains were observed, travelling one behind the other with different wavelengths (periods) and different (initial) phase speeds (although they all ended with a phase speed of about 600 km s^{-1}. Comparisons between these waves and the radio spectrum of the flare acquired from the *Nançay Radioheliograph (NRH)* revealed that each wave train was triggered by a burst of radio energy caused by the acceleration of non-thermal electrons above the magnetic reconnection site. The periods of such waves follow a characteristic "tadpole" pattern, where the period decreases at a fixed height, which is 150 Mm here.

Could possibly be the kink mode if waveguide was in the form of a loop. These can only be identified if the observed loop segment has a certain line of sight with respect to the observer, and a longer wavelength results in a faster speed, which then results in the dispersion of fast magnetoacoustic waves. The range in propagating phase speeds they derived was $v_{ph} = 735 - 845$ km s^{-1}, with a final speed (post-dispersion) of 600 km s^{-1}.

3.6. Torsional Modes

Torsional modes, or more commonly, *Alfvén* modes, are axisymmetric modes whose speed is determined purely by magnetic pressure forces (see equation 2). They are transverse waves that are highly anisotropic (Goossens (2003)), with a *group* speed that travels strictly along magnetic field lines in response to a restoring force that acts to resist shear (cite class notes?). The *phase* speed can be at an angle θ to the direction of the magnetic field $\vec{B}$:

$$V_A = \pm \frac{B}{\sqrt{4\pi\rho}} \cos\theta \tag{7}$$

The energy carried by this wave is contained in the group speed (Somov (2013)... this source also has a good phase velocity diagram).

In the classic cylindrical model of a plasma structure, Alfvén waves undergo torsion (aka, twisting), in opposite directions on either end of the cylinder (Nakariakov & Verwichte (2005)).

The primary damping mechanism for Aflvén waves is resonant absorption, and is thought to be a possible cause for coronal heating (?).

Tian et al. (2012) used spectroscopic observations of the Fe XII λ 195.12 line to investigate Doppler shifts along the line-of-sight (LOS) in a coronal loop. They found that oscillations do not necessarily indicate MHD waves, as these same oscillations can result from upflows of jets, which were found to be the dominate source of the oscillations seen around the loop footpoints. Toward the top of the loop, the observed oscillations were in fact found to be due to either kink or Alfvén waves (both are fast waves that do not cause density perturbations, and hence are not observed by intensity oscillations... other similarities?) They also noted that intensity changes can occur as a result of the loop itself begin in motion, transversing back and forth across the slit location, and cautioned that a phase difference between intensity and Doppler shift was not an immediate indication of density perturbation, and further analysis should be carried out.

Alfvén waves can be difficult to observe (or at least difficult to identify observed disturbances as Alfvén waves) since, like kink oscillations, they do not cause any periodic changes in intensity or density. It follows that determining the Alfvén speed is also difficult, depending on what parameters are directly observable. Verwichte et al. (2013) derived the Alfvén speed using using seismological techniques and compared this to the one measured from direct observation of two coronal loops whose oscillations were triggered by an X-class flare. They showed that there is a three-way interplay between seismology, magnetic extrapolation, and spectroscopy. Since the Alfvén speed, V_A is determined by density and magnetic field:

$$V_A \propto B\rho^{-1/2} \tag{8}$$

3.7. Mixed Modes

4. Discussion

The observational techniques and relevant properties of each of the different kinds of MHD waves are summarized in table 1.

5. Data

As part of the general topic of coronal seismology, a small research project was carried out as well, continuing over from several semesters previously. Several of the observational and analytical methods used in the literature were reproduced for this project.

6. Analysis

7. Conclusion

And we're finished.

REFERENCES

Asai, A., Ishii, T. T., Isobe, H., et al. 2012, ApJ, 745, L18

Aschwanden, M. 2004, Physics of the Solar Corona: An Introduction

Aschwanden, M. J., Fletcher, L., Schrijver, C. J., & Alexander, D. 1999, The Astrophysical Journal, 520, 880

Goossens, M. 2003, An Introduction to Plasma Astrophysics and Magnetohydrodynamics, Vol. 294 (P.O. Box 17, 3300 AA Dordrecht, The Netherlands: Kluwer Academic Publishers)

Lopin, I., & Nagorny, I. 2015, ApJ, 810, 87

Morton, R. J., Erdélyi, R., Jess, D. B., & Mathioudakis, M. 2011, ApJ, 729, L18

Nakariakov, V. M., & Verwichte, E. 2005, Living Rev. Solar Phys.

Pascoe, D. J., Wright, A. N., De Moortel, I., & Hood, A. W. 2015, A&A, 578, A99

Robbrecht, E., Verwichte, E., Berghmans, D., et al. 2001, A&A, 370, 591

Roberts, B., Edwin, P. M., & Benz, A. O. 1984, ApJ, 279, 857

Somov, B. V. 2013, Plasma Astrophysics, Part I: Fundamentals and Practice, 2nd edn.

Srivastava, A. K., & Dwivedi, B. N. 2010, MNRAS, 405, 2317

Tian, H., McIntosh, S. W., Wang, T., et al. 2012, ApJ, 759, 144

Uritsky, V. M., Davila, J. M., Viall, N. M., & Ofman, L. 2013, ApJ, 778, 26

Verwichte, E., Van Doorsselaere, T., Foullon, C., & White, R. S. 2013, ApJ, 767, 16

Yuan, D., Shen, Y., Liu, Y., et al. 2013, A&A, 554, A144

This 2-column preprint was prepared with the AAS LaTeX macros v5.2.

Type of wave	Timescales	Sizescales	Observational techniques
Kink Oscillations	short	short	something
Sausage Oscillations	short	short	something
Acoustic Oscillations	x	x	x
Propagating	x	x	x